

Structural, electrical, magnetic, and optical properties of bis-benzene-1,2-dithiolato-Au(IV) crystals

N. C. Schiødt, T. Bjørnholm,* and K. Bechgaard[†]

Centre for Interdisciplinary Studies of Molecular Interactions, Department of Chemistry, Symbion Science Park, University of Copenhagen, Fruebjergvej 3, DK-2100 Ø, Copenhagen, Denmark

J. J. Neumeier[‡] and C. Allgeier[§]

Sektion Physik der Ludwig-Maximilian Universität, Schellingstrasse 4/IV, 80799 München, Germany

C. S. Jacobsen

Physics Department, Technical University of Denmark, DK-2800, Lyngby, Denmark

N. Thorup

Structural Chemistry Group, Chemistry Department B, Technical University of Denmark, DK-2800, Lyngby, Denmark

(Received 18 May 1995)

Analysis of x-ray diffraction from a single crystal of bis-benzene-1,2-dithiolato-Au(IV) [Au(bdt)₂] at 125 K reveals a superstructure along the stacks of Au(bdt)₂ molecules corresponding to a dimerization of the molecules along the stack. Within a dimer, intermolecular sulfur-sulfur contacts are shortened from 3.7 to 3.6 Å whereas a lengthening to about 3.8 Å is found between dimers. Electrical resistivity measured by a four-probe method between 230 and 450 K uncovers an activated resistivity with a characteristic energy of 0.30 eV. The room-temperature conductivity at zero applied pressure is 0.11 Ω⁻¹ m⁻¹ rising smoothly to 0.67 Ω⁻¹ m⁻¹ at 0.55 GPa isotropic pressure. The magnetic susceptibility χ is low compared to the spin susceptibility of a system with one free spin per molecule. An activated behavior of χ is observed, which gives rise to a monotonic increase in χ at between 275 and 420 K. Reflectivity measurements along the *b* axis (stacking direction) of a single crystal of Au(bdt)₂ shows a transition around 5000 cm⁻¹ (0.6 eV) possessing an oscillator strength ≈0.5 electron/molecule. Along the *c* axis an absorption centered around 8000 cm⁻¹ is observed. The first transition (5000 cm⁻¹) is attributed to an intermolecular charge-transfer process while the latter transition (8000 cm⁻¹) most likely corresponds to an intramolecular excitation. The physical data presented are discussed in the context of a soft Mott insulator.

INTRODUCTION

The transition-metal dithiolene complexes have been intensively studied for more than 25 years since they possess extraordinary redox behavior, molecular geometry, and physical properties.¹⁻⁵ Within this family the Ni- and Cu-group dithiolenes are all planar and exhibit a wide range of physical behavior, including metallicity and superconductivity.⁶ An example of the latter is the well-known tetrathiafulvalene (TTF₂) Ni(dmit)₂, where dmit denotes 4,5-dimercapto-1,3-dithiole-2-thione.⁷

The gold-dithiolene complexes—though much less studied than the Ni dithiolenes—are known in a range of oxidation states.⁸⁻¹⁹ As shown in the present paper, the odd-electron compound bis-(benzene-1,2-dithiolato)-gold [Au(bdt)₂] belongs to the group of planar molecules, which in the solid state form electrically (semi)conducting molecular stacks with a half-filled electronic band. A more well-known member of this group is K-TCNQ (tetracyanoquinodimethane).²⁰ However, Au(bdt)₂ is unique since it is a neutral, odd-electron species. X-ray structure determination reveals nearly uniform stacks of Au(bdt)₂ molecules with a weak superstructure.¹⁷ *Ab initio* calculations on the isolated Au(bdt)₂ molecule show the highest occupied and singly occupied molecular orbitals (HOMO and SOMO)

to be almost the pure bonding and antibonding combinations of the ligand HOMO's, and also to be very close in energy.²¹ This indicates that the central gold atom provides only a weak coupling between the two ligands; much the same situation as in the Ni(dmit)₂-type species.^{22,23}

We report here the electrical, optical, and magnetic properties of single crystals of the title compound Au(bdt)₂. The results show that the physical properties such as resistivity and magnetism are dominated by electron-electron correlations.

EXPERIMENT

Au(bdt)₂ was prepared by electrocrystallization of (C₄H₉)₄N⁺ Au(bdt)₂⁻ as reported in the literature.¹⁷ (C₄H₉)₄N⁺ Au(bdt)₂⁻ was prepared as described in Ref. 21.

A single crystal (0.24×0.09×0.05 mm³) was used for x-ray analysis at around 125 K. Weissenberg photographs showed considerable condensation of the previously reported superstructure reflections associated with a doubling of the *b* axial length.¹⁷ A CAD-4 diffractometer was used for unit cell determination and collection of intensity data. The crystal symmetry is monoclinic, space group *Pn* (*P*2₁/*n* in subcell) with *a*=12.335(6) Å, *b*=7.409(3) Å, *c*=14.469(7) Å, β =112.08(5)°, *V*=1225.3(3) Å³, μ (Mo *K*α)=125.9 cm⁻¹.

2435 reflections were measured with ω scan in the range $0 < \theta < 25^\circ$, $-14 < h < 14$, $0 < k < 8$, $0 < l < 17$. Data reduction gave 2245 unique reflections, of which 1967 had $I > 2\sigma(I)$ and were used in subsequent refinements. Corrections for Lorentz, polarization, and absorption effects (transmission 0.32–0.55) were applied. Initial atomic coordinates were taken from the room-temperature structure study (average structure in subcell) and used for refinement in a 125-K subcell with $b = \frac{1}{2} \times 7.409 \text{ \AA}^2$. This refinement converged with residuals $R = 0.025$ and $wR = 0.034$ with anisotropic thermal parameters for all atoms (H atoms were ignored). Refinements in the larger cell were also attempted, but unconstrained refinements were hampered by severe correlations due to the weakness of reflections with k odd. Therefore, the two independent molecular radicals were refined as rigid bodies with fixed geometry from the 125-K average structure but allowing for translation and rotation of each radical. Atoms of the same kind were assigned a common isotropic thermal parameter. This procedure led to final residuals $R = 0.055$ and $wR = 0.072$ with 14 parameters. The resultant individual atomic coordinates are not reported since they were derived from a highly constrained refinement. The crystallographic programs used were SHELX76,²⁴ PLATON,²⁵ and PLUTO.²⁶

Electrical resistivity in the temperature range 235 K $< T < 460$ K was measured using a four-point method whereby reversal of the current direction at each measured temperature cancels thermal voltages. Typical currents used for this measurement were $5.7 \text{ mA/cm}^2 \leq J \leq 30 \text{ mA/cm}^2$. Four well-annealed Pt wires with a diameter of 3 μm were fixed to a nonconducting surface with GE varnish in a configuration of comparable geometry to the sample. The leads were contacted to the sample using silver paint where the original thinner was replaced by octyl-acetate, which slows the drying process. The temperature was measured with a Pt thermometer in the range 235 K $< T < 295$ K and a Pt-Rh thermocouple in the range of 295 K $< T < 460$ K. Measurements at high pressures were carried out in a He-gas medium. Pressure was generated with a commercially available He-gas compressor. Static magnetic susceptibility was measured in a Faraday magnetometer in an applied magnetic field of 5.7 T. A gold-plated high-purity copper crucible suspended from the microbalance on a Pt wire was used as a sample holder for the randomly oriented 50.15-mg quantity of single crystals. The magnetic susceptibility of the crucible and the suspension was measured and subtracted from the data. After the sample had been placed in the crucible and suspended in the magnetometer, the sample region was evacuated for 15 h followed by the admission of 1 mbar of pure He gas. Observation of the sample-region atmosphere with a quadrupole mass spectrometer ensured that an oxygen concentration of less than 2×10^{-8} mbar was present during the entire measurement. Data were acquired during thermal drift from 330 to 4 K at a rate of 1 K/min. Data above 330 K were taken while heating the sample region at a rate of 1 K/min with a noninductive furnace mounted in the cryostat.

The single-crystal reflectance of infrared and visible wavelengths was measured at 300 K on a $0.3 \times 1.0 \text{ mm}^2$ (100) face. A single-beam monochromator with gratings for the infrared and a quartz prism for the visible in connection with global and halogen lamps provided the radiation, while

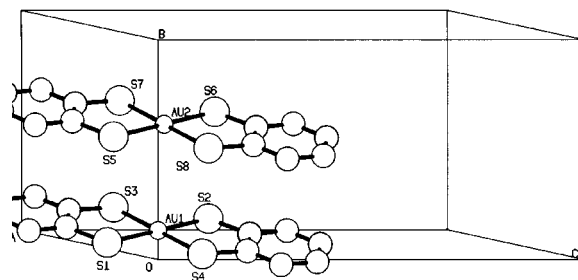


FIG. 1. Side view showing two independent radicals in the stack along b . Unlabeled atoms are carbon atoms.

the appropriate polarization was selected with wire grid and calcite prism polarizers in the two spectral ranges. An aluminum mirror served as reference taking into account the finite reflectance of Al.

RESULTS AND DISCUSSION

The average crystal structure of $\text{Au}(\text{bdt})_2$ consists of stacks of the neutral radicals along the b axis (Fig. 1).¹⁷ All short intrastack $S \cdot S$ contacts are identical and equal to b (subcell), i.e., 3.75 \AA at room temperature and 3.70 \AA at 125 K. A somewhat short intermolecular $S \cdot S$ contact (3.66 and 3.6 \AA at the two temperatures, respectively) connects a stack along b going through the origin with an equivalent and parallel stack through the center of the unit cell. The stacks are thus weakly connected to form layers defined by directions $[010]$ and $[101]$. At room temperature very weak intensity reflections corresponding to a supercell with $b = 7.500 \text{ \AA}$ can be observed. On Weissenberg photographs these reflections are very elongated along the $-\mathbf{a}^* + \mathbf{b}^*$ direction, but at lower temperature they become more intense and less elongated. This suggests a dimerization in the stack direction with incomplete long-range correlation between the stacks. In the present analysis all observed reflections at 125 K corresponding to a unit cell having $b = 7.406 \text{ \AA}$ were included in structure refinement. Although highly constrained (see experimental part), the refinement with all reflections clearly indicate that the alternating radicals in a stack are mainly subject to relative translations. The atom Au2 in Fig. 1 is displaced from its "ideal" position $(0, \frac{1}{2}, 0)$ relative to Au1 by -0.12 , -0.11 , and 0.16 \AA along a , b , and c , respectively. The two neighboring radicals in a stack are no longer strictly parallel and the interplanar distance is thus not well defined. A dimerization is clearly seen when considering the intrastack $S \cdot S$ distance. Within a dimer these contacts are shortened from 3.70 \AA to about 3.6 \AA , whereas a lengthening to about 3.8 \AA is found between the dimers. The short interstack distance of 3.6 \AA is unchanged by the distortion. The absence of strong interactions along the $[-101]$ direction may explain the apparent incomplete correlation between stack dimerizations.

Resistivity as a function of temperature is displayed in Fig. 2. An activated behavior typical of a semiconductor is observed. Assuming that $R(T) = A \exp(-\Delta/kT)$, an activation energy $\Delta = 0.30 \text{ eV}$ is found from the slope of the plot shown in Fig. 2. In a band description this corresponds to a band gap of 0.60 eV. The room-temperature conductivity measured along the stacking direction is $0.11 \text{ } \Omega^{-1} \text{ m}^{-1}$.

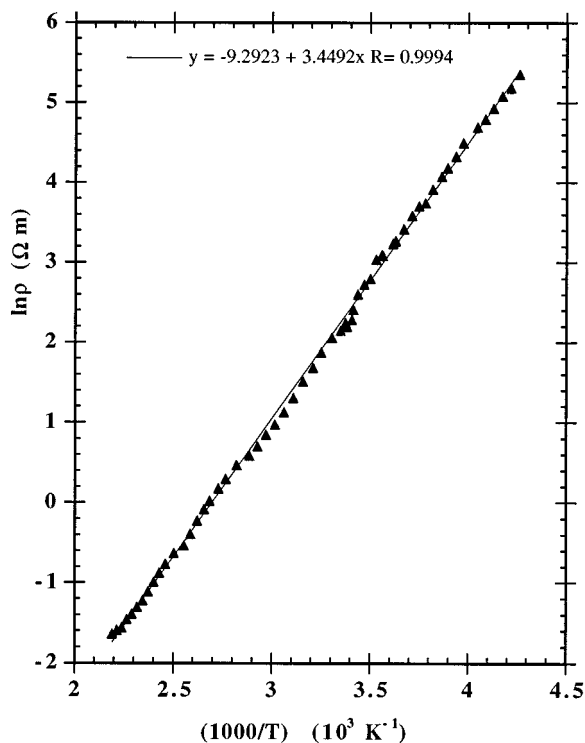


FIG. 2. Resistivity along stacking direction vs temperature of $\text{Au}(\text{bdt})_2$ single crystal.

In general, organic compounds possess rather large compressibilities which suggests that the transport properties should also be strongly pressure dependent. The electrical resistivity at 295 K under purely hydrostatic pressure is shown in Fig. 3, where the filled and open symbols indicate data taken while increasing and decreasing the pressure, respectively. The curve can be fitted with a polynomial of third order given by

$$\rho(P) = 9.46 - 39.29P + 74.91P^2 - 55.99P^3 \quad \Omega \text{ m}. \quad (1)$$

The initial slope at $P \approx 0$ is given by $(d\rho/dP)_{P=0} = -39.29 \text{ } \Omega \text{ m/GPa}$. At the highest pressure attained of $P = 0.54 \text{ GPa}$ the electrical resistivity of $\text{Au}(\text{bdt})_2$ has reached $\rho(0.54 \text{ GPa}) = 1.3 \text{ } \Omega \text{ m} = 1.3 \times 10^5 \text{ m}\Omega \text{ cm}$. For comparison, the electrical resistivities at 300 K and at an atmospheric pressure of the highly conducting organic compounds TTF-TCNQ, HMTTF-TCNQ, TSF-TCNQ, HMTSF-TCNQ, and HMTSF-TNAP are 2.5, 1.88, 1.23, 0.53, and 0.50 $\text{m}\Omega \text{ cm}$, respectively.²⁷ It is clear that we are a long way from values typical of organic metals. However, we point out that the electrical resistivity of this compound is fairly pressure sensitive decreasing by over 85% with only 0.54 GPa of pressure. For comparison, the pressure dependence²⁷ of TTF-TCNQ is $d \ln \rho/dP \approx -280\% \text{ GPa}^{-1}$. We note that this is smaller than the initial slope of $d \ln \rho/dP \approx -416\% \text{ GPa}^{-1}$ which we observe in $\text{Au}(\text{bdt})_2$. If an average of the $d \ln \rho/dP$ along the curve in Fig. 3 at the points 0, 0.1, 0.2, 0.3, 0.4, and 0.5 GPa is taken using Eq. (1), we obtain $(d \ln \rho/dP)_{\text{avg}} \approx -375\% \text{ GPa}^{-1}$. Using this value the pressure where the electrical resistivity would attain $10^{-3} \text{ } \Omega \text{ cm}$ in $\text{Au}(\text{bdt})_2$ is estimated as 3.7 GPa. Unfortunately, the pressure

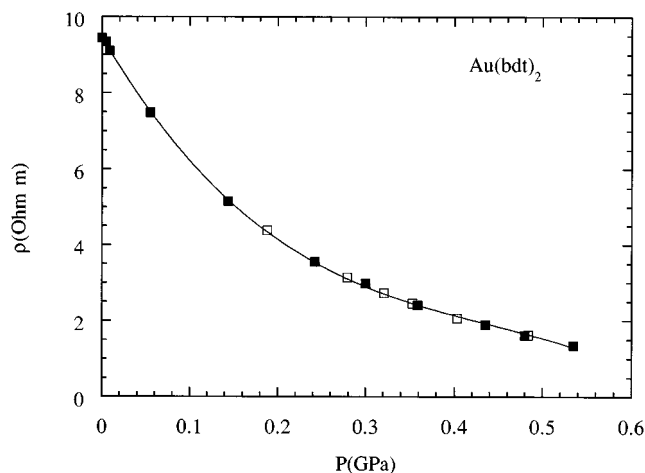


FIG. 3. Electrical resistivity at 295 K vs purely hydrostatic pressure of $\text{Au}(\text{bdt})_2$. The filled symbols and open symbols indicate data obtained while increasing and decreasing the pressure, respectively.

range of our apparatus is below 0.7 GPa so it was not possible for us to investigate the properties of this compound at higher pressures.

The measured magnetic susceptibility vs temperature of $\text{Au}(\text{bdt})_2$ is displayed in Fig. 4. These data are corrected for the diamagnetism of $\text{Au}(\text{bdt})_2^-$ by using the room-temperature magnetic susceptibility of $(\text{C}_4\text{H}_9)_4\text{N}^+\text{Au}(\text{bdt})_2^-$ and $(\text{C}_4\text{H}_9)_4\text{N}^+\text{Br}^-$, which was measured in conjunction with this project, and the tabulated value of the diamagnetism of Br^- obtained from the standard tables.²⁸ This yielded the correction $\chi_{\text{dia}} = -2.0 \times 10^{-4} \text{ cm}^3/\text{mol}$.

If one compares the magnitude of the observed susceptibility at 300 K to that of an imaginary system with one free localized spin per $\text{Au}(\text{bdt})_2$ molecule ($1.25 \times 10^{-3} \text{ cm}^3/\text{mol}$), the measured value of χ is found to be 14 times smaller than that of the imaginary system. When the temperature dependence of this imaginary system is assumed to be Curie-Weiss-like, this difference in χ is magnified many times with a reduction of temperature. This comparison is made in order to illustrate the rather weak magnetism of $\text{Au}(\text{bdt})_2$. We can

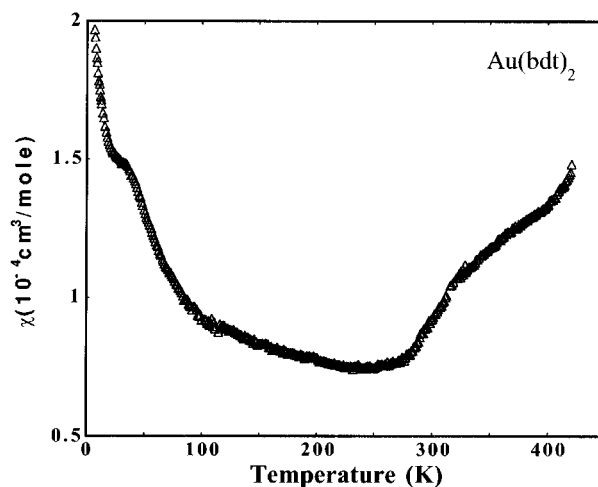


FIG. 4. Static magnetic susceptibility vs temperature of $\text{Au}(\text{bdt})_2$. The data are corrected for core diamagnetism.

therefore with confidence assume that the magnetic behavior is much weaker and more complicated than that of a simple magnetic analogue with one free spin per molecule.

We have considered various possibilities in order to understand the increase of magnetic susceptibility with temperature above $T \sim 275$ K. A semiconductorlike magnetic susceptibility, for example, can climb exponentially with temperature due to excitation of charge carriers into the conduction band.²⁹ Using the energy gap derived from our electrical resistivity measurements the strong observed upturn in χ can be obtained when an effective mass for the charge carriers of $500m_e$, where m_e is the mass of the electron, is chosen. The anomalously large effective mass suggests that this description is unphysical.

Another possibility is to consider antiferromagnetic ordering. The drop in χ with decreasing temperature in the high-temperature region indicates that the system may be dominated by antiferromagnetic interactions already at the high-temperature end of our measurement. Since our structural data show that this high-temperature part of the magnetic susceptibility is little affected by dimerization a Bonner-Fischer-type magnetism describing a one-dimensional antiferromagnetic chain may be in accordance with the experimental data.³⁰ According to Bonner and Fischer, the temperature T_{\max} where the maximum magnetic susceptibility χ_{\max} is reached is given by $1.28J/k$ (K) where J represents the antiferromagnetic exchange coupling between adjacent sites, and k_B is Boltzmann's constant. The value χ_{\max} is $0.11k_B/J$ ($\text{K}^{-1} \text{cm}^3/\text{mol}$).³¹ Assuming that the system is highly correlated (Hubbard $U \approx 4t$) we can estimate the value of J by using³¹ $J \approx 2t^2/U$, where $U \approx 0.6$ eV comes from optical data (see below) and t is estimated to 0.12 eV by comparison to analogous TCNQ salts. This gives $T_{\max} = 700$ K and $\chi_{\max} = 2 \times 10^{-4} \text{cm}^3/\text{mol}$. A peak at 700 K with maximum at $2 \times 10^{-4} \text{cm}^4/\text{mol}$ cannot be confirmed by the experimental data due to phase separation of the crystals when heated to temperatures above 420 K. The relatively rapid drop in the susceptibility in the region between 420 and 300 K is, however, not expected from a simple Bonner-Fischer-type model and it is hence likely that the dimerizing of the lattice has a pronounced effect on the magnetism even in this high-temperature region. The dimerization could be the signature of a spin Peierls transition or "generalized" Peierls transitions as suggested for similar systems [e.g., KTCNQ (Ref. 32) and HMTTF-TCNQF₄ (Ref. 33)].

We note that the low-temperature part of the magnetic susceptibility may contain contributions from soliton-antisoliton pairs in analogy with polyacetylene³⁴ in addition to possible paramagnetic impurities. Further investigation of the magnetic anisotropy on single crystals and with neutron diffraction may provide more details concerning the magnetic state of this system.

Figure 5 presents the measured room-temperature reflectance spectra. The *b*-axis (stacking-axis) spectrum was determined in the range 2400–18 000 cm^{-1} , while the *c*-axis (along the long axis of the molecules) spectrum was measured from 4000 to 18 000 cm^{-1} . The *b*-axis spectrum looks "metallic" with a plasma-edge-type feature at 10 000–13 000 cm^{-1} . However, the level off in reflectance towards the low-frequency end indicates that the spectrum is dominated by a strong oscillator at finite frequency which physi-

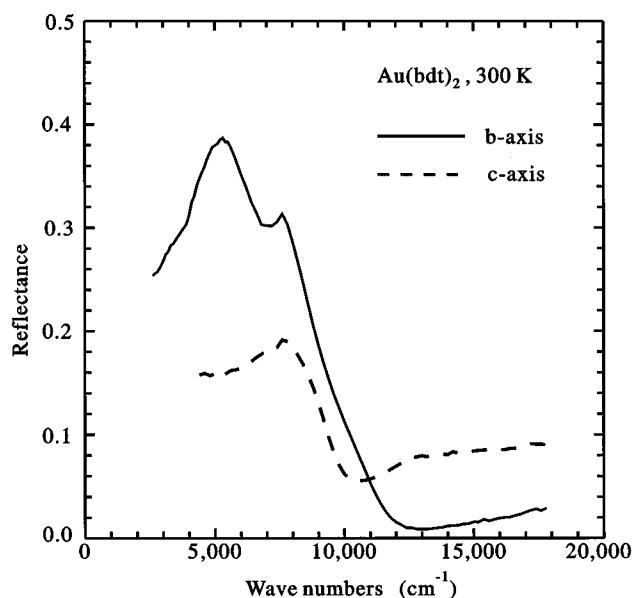


FIG. 5. Polarized reflectance of a single crystal of $\text{Au}(\text{bdt})_2$ at 300 K. Solid line: *b* axis. Dashed line: *c* axis.

cally must originate from the charge-transfer (CT) excitations. A weaker feature is superimposed on this resonance. In the other polarization direction, a single oscillator on a dielectric background is observed.

In order to further extract information from the spectra, a Kramers-Kronig transformation³⁵ was performed. Since this scheme requires knowledge of the spectra in the entire frequency range, the low-frequency reflectance below the measured range was assumed constant, while a smooth connection in the high-frequency end was made to join standard extrapolation schemes.³⁵ The spectral features in the measured range are not very sensitive to the precise choice of extrapolations. Figure 6 shows the results of the transformation in terms of the optical conductivity. As expected, the *b*-axis spectrum has a dominant peak with weaker shoulders superimposed. As indicated above, the resonance must be attributed to a charge-transfer process between molecules along the stacks. The position of the peak at 5000 cm^{-1} corresponds to a photon energy of 0.6 eV, which matches the band gap estimated from the resistance measurements. The area below the peak in conductivity corresponds to the oscillator strength of the transition. Taking into account the unit cell volume and the presence of two molecules per unit cell, this oscillator strength is found to correspond to 0.4–0.5 electron per $\text{Au}(\text{bdt})_2$ molecule. Such a number is quite typical for the low-lying valence electron charge-transfer transitions in molecular crystals.³⁶

The *c*-axis spectrum shows a resonance at 8000 cm^{-1} . Since this polarization is roughly parallel to the long axis of the molecules, we associate this transition with the lowest-lying intramolecular transition in $\text{Au}(\text{bdt})_2$. This transition is expected for an isolated $\text{Au}(\text{bdt})_2$ molecule since $\text{Au}(\text{bdt})_2$ is isoelectronic with the well characterized $\text{Ni}(\text{bdt})_2^-$ complexes possessing intense near-infrared transitions due to $\pi-\pi^*$ transition in the ligands.²¹ Another possibility is a charge-transfer transition between molecules in adjacent stacks. This interaction could be mediated by the short

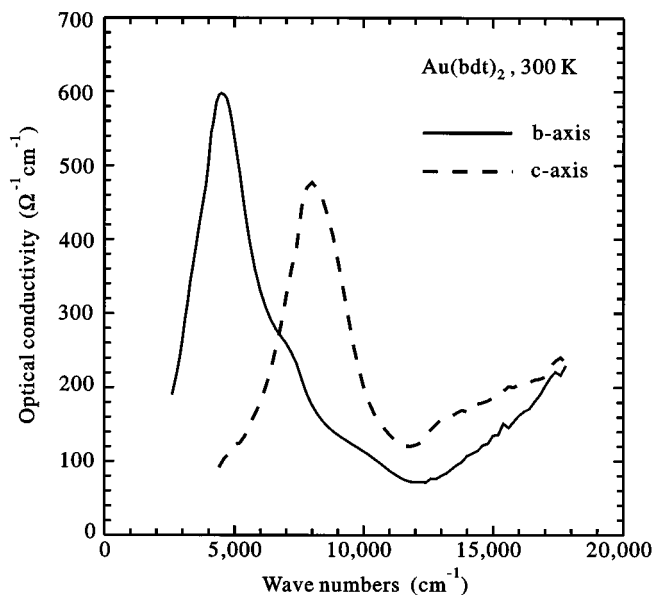


FIG. 6. Optical conductivity of $\text{Au}(\text{bdt})_2$ as obtained by Kramers-Kronig transformation of the data in Fig. 5. Solid line: b axis. Dashed line: c axis.

sulfur-sulfur interstack contact; however, it should be expected to be considerably weaker than the intrastack interaction. Since the oscillator strength of the transitions is proportional to the intermolecular interactions, the interstack CT should hence be considerably less intense than the intrastack CT transitions. This does not agree with the observed transitions of roughly equal oscillator strength and we therefore consider it most plausible to assign the peak at 8000 cm^{-1} to

an intramolecular π - π^* excitation as described above. The shoulders in the b -axis spectrum around this position could reflect that the intramolecular transition mixes with the intrastack charge-transfer excitation.

CONCLUSIONS

At high temperature crystals of $\text{Au}(\text{bdt})_2$ consist of nearly uniform stacks of neutral molecular radicals with one charge carrier per molecule. The packing motif indicates that electronic interactions in the crystal are by far most efficient along the stacking direction of the molecules (b direction). At low temperatures a weak dimerization develops. The weak dimerization as well as discrepancies between the observed magnetic and optical properties and simple (uncorrelated) band theory indicates that the system is most accurately described in a strong coupling limit (Hubbard $U \approx 4t$). Following this analysis, the observed activation energy for conduction is found to be roughly equal to the on-site Coulomb repulsion (U) found by optical methods ($E_g \approx U = 0.6\text{ eV}$) as expected in the strong coupling limit. These values together with a reasonable estimate of the transfer integral (t) bring the high temperature part of the magnetic susceptibility in fair agreement with the expected behavior of an anti-ferromagnetically coupled one dimensional chain with one spin per site. The physical properties are in many respects very similar to KTCNQ.²⁰

ACKNOWLEDGMENTS

This work was supported by the Danish Materials Research Program (MUP) and the Deutsche Forschungsgemeinschaft under Grant "Schi.208/1-4." Professor Canadell is gratefully acknowledged for inspiring discussions regarding the electronic structure of $\text{Au}(\text{bdt})_2$.

* Author to whom correspondence should be addressed.

[†] Present address: MST-10, Mail Stop k764, Los Alamos National Laboratory, Los Alamos, NM 87545.

[‡] Present address: Osram GmbH, Hellabrunner Str. 1, 81543, München, Germany.

[§] Present address: Physics Department, RISØ National Laboratory, P.O. Box 49, DK-4000 Roskilde, Denmark.

¹ J. A. McCleverty, *Prog. Inorg. Chem.* **10**, 29 (1968).

² R. P. Burns and C. A. McAuliffe, *Adv. Inorg. Chem. Radiochem.* **22**, 303 (1979).

³ C. Mahadevan, *J. Cryst. Spectrosc. Res.* **16**, 347 (1986).

⁴ E. Hoyer, W. Dietzsch, H. Müller, A. Zschunke, and W. Schroth, *Inorg. Nucl. Chem. Lett.* **3**, 457 (1967).

⁵ H. B. Gray, *Trans. Met. Chem.* **1**, 239 (1965).

⁶ J. A. Ibers, L. J. Pace, J. Martinsen, and B. M. Hoffman, *Struct. Bond.* **50**, 1 (1982).

⁷ L. Brossard, M. Bousseau, M. Ribault, L. Valade, and P. Cassoux, *C. R. Acad. Sci. Paris* **302**, 205 (1986).

⁸ J. H. Waters and H. B. Gray, *J. Am. Chem. Soc.* **87**, 3534 (1965).

⁹ J. G. M. Van Rens, M. P. A. Vieggers, and E. DeBoer, *Chem. Phys. Lett.* **28**, 104 (1974).

¹⁰ R. L. Schlupp and A. H. Maki, *Inorg. Chem.* **13**, 44 (1974).

¹¹ J. J. Jenkins, Ph.D. thesis, Howard University, 1976.

¹² A. Davison, N. Edelstein, R. H. Holm, and A. H. Maki, *Inorg. Chem.* **2**, 1227 (1963).

¹³ R. Williams, E. Billig, J. H. Waters, and H. B. Gray, *J. Am. Chem. Soc.* **88**, 43 (1966).

¹⁴ M. J. Baker-Hawkes, E. Billig, and H. B. Gray, *J. Am. Chem. Soc.* **88**, 4870 (1966).

¹⁵ A. Davison, D. V. Howe, and E. T. Shawl, *Inorg. Chem.* **6**, 458 (1967).

¹⁶ J. Schultz, H. H. Wang, L. C. Soderholm, T. L. Sifter, J. M. Williams, K. Bechgaard, and M. Whangbo, *Inorg. Chem.* **26**, 3757 (1987).

¹⁷ G. Rindorf, N. Thorup, T. Bjørnholm, and K. Bechgaard, *Acta Crystallogr. Sec. C* **46**, 1437 (1990).

¹⁸ N. C. Schiødt, T. Bjørnholm, C. S. Jacobsen, and K. Bechgaard, *Synth. Met.* **56**, 2164 (1993).

¹⁹ E. B. Yagubskii, A. I. Kotov, E. E. Laukhina, A. A. Ignatiev, L. I. Buravov, A. G. Khomenko, V. E. Shklover, S. S. Nagapetyan, and Yu. T. Struchkov, *Synth. Met.* **42**, 2515 (1991).

²⁰ See, e.g., M. Konno, T. Ishii, and Y. Saito, *Acta Crystallogr. Sec. B* **33**, 763 (1977); M. Meneghetti, *Phys. Rev. B* **44**, 8554 (1991).

²¹ N. C. Schiødt, P. Sommer-Larsen, T. Bjørnholm, M. Folmer Nielsen, J. Larsen, and K. Bechgaard, *Inorg. Chem.* **34**, 3688 (1995).

²² E. Canadell, S. Ravy, J. P. Pouget, and L. Brossard, *Solid State Commun.* **75**, 633 (1990).

²³ E. Canadell, I. E.-I. Rachidi, S. Ravy, J. P. Pouget, L. Brossard, and L. P. Legros, *J. Phys. (Paris)* **50**, 2967 (1989).

- ²⁴G. M. Sheldrick, SHELX76 computer program for crystal structure determination, University of Cambridge, 1976.
- ²⁵A. L. Spek, *Acta Crystallogr. Sect. A* **46**, C-34 (1990).
- ²⁶W. D. Motherwell and W. Clegg, PLUTO computer program for plotting molecular and crystal structures, University of Cambridge, 1978.
- ²⁷D. Jérôme and H. J. Schulz, *Adv. Phys.* **31**, 299 (1982).
- ²⁸*CRC Handbook of Chemistry and Physics*, 53rd ed. (CRC, Boca Raton, FL, 1973).
- ²⁹S. V. Vonsovskii, *Magnetism* (Wiley, New York, 1974), Vol. I, p. 275.
- ³⁰J. C. Bonner and M. E. Fisher, *Phys. Rev.* **135**, A640 (1964).
- ³¹See, e.g., Z. G. F. Soos, *Annu. Rev. Phys. Chem.* **25**, 121 (1974).
- ³²J. G. Vegter and J. Kommandeur, *Mol. Cryst. Liq. Cryst.* **30**, 11 (1975).
- ³³J. B. Torrance, Y. Tomkiewicz, R. Bozio, C. Pecile, C. R. Wolfe, and K. Bechgaard, *Phys. Rev. B* **26**, 2267 (1982).
- ³⁴I. B. Goldberg, R. H. Crowe, P. R. Newman, A. J. Heeger, and A. G. MacDiarmid, *J. Chem. Phys.* **70**, 1132 (1979); for a review see, e.g., S. Roth and H. Bleier, *Adv. Phys.* **36**, 385 (1987).
- ³⁵See, for example, F. Wooten, *Optical Properties of Solids* (Academic, New York, 1972), p. 244.
- ³⁶See, for example, C. S. Jacobsen, in *Highly Conducting Quasi-One-Dimensional Solids*, edited by E. M. Conwell, *Semiconductors and Semimetals Vol. 27* (Academic, New York, 1988), p. 293.